Magnetic Resonance Dowsing

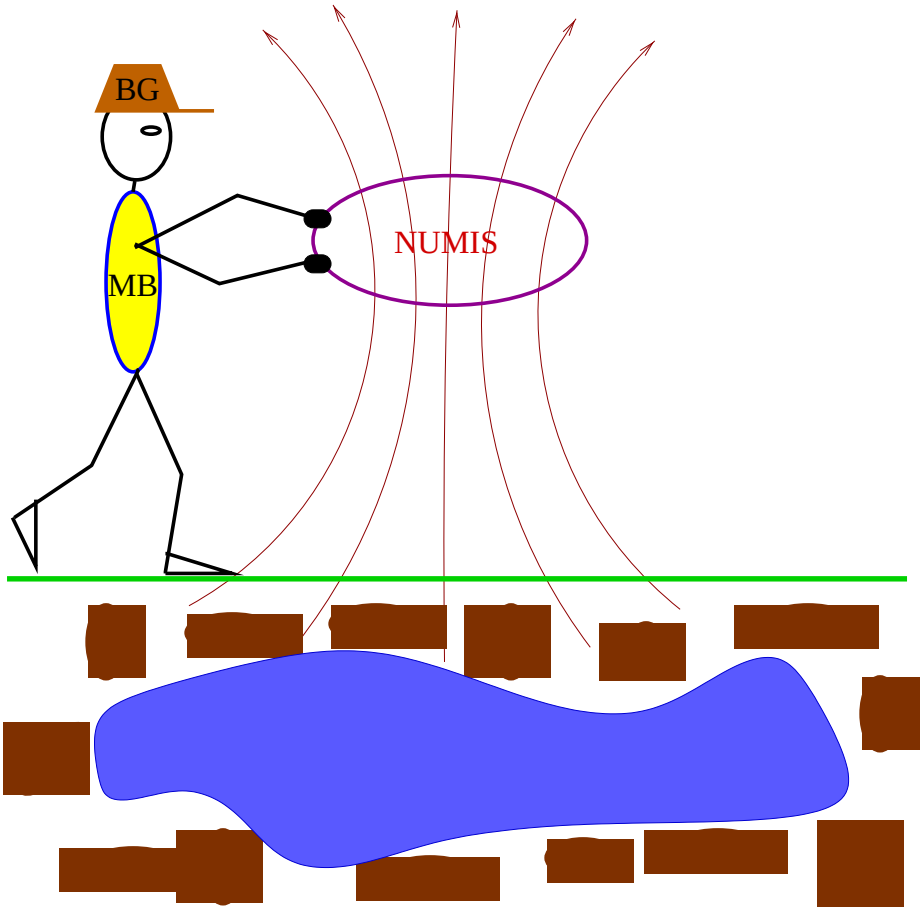

Peter B. Weichman, Eugene M. Lavely
Blackhawk Geometrics

Michael H. Ritzwoller
Department of Physics, CU Boulder

Research funded by the DOE
Talk prepared with LaTeX2$_\varepsilon$

The Holy Grail

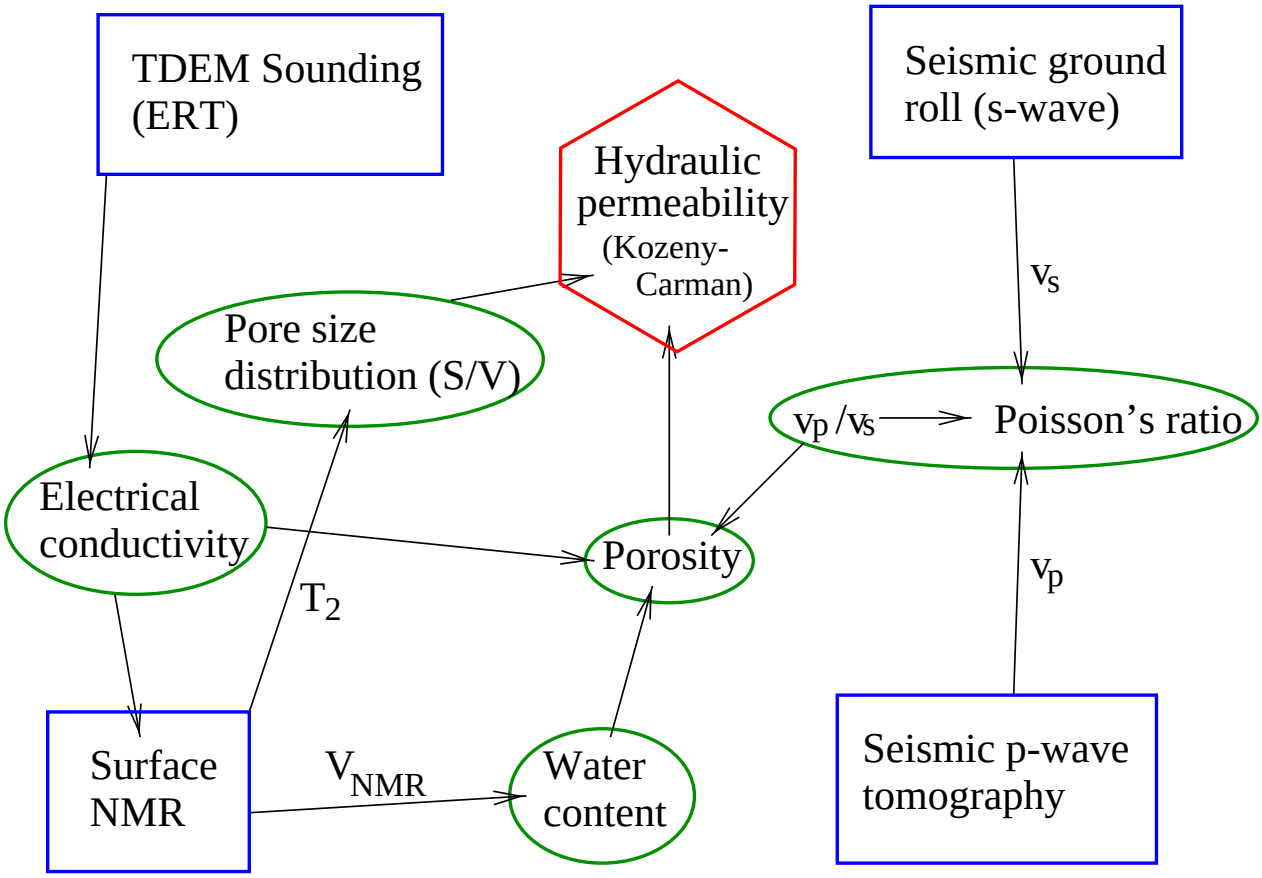

The aim is to develop a 3D tomographic method capable of inferring hydro-geological parameters, important to contaminant transport modeling, with 2-5 meter resolution by combining seismic (U. Colorado, Geotomo), TDEM (Blackhawk, Geotomo) and surface NMR (Blackhawk, JPL) measurements.

Each method yields important, interdependent partial information with varying resolution. A full joint inversion is required to obtain the needed hydro-geological data.

A Little History

Initial Idea: R. H. Varian, 1962, *Ground liquid prospecting method and apparatus*, U.S. Patent 3,019,383.

First successful prototype: Scientists at the Institute for Chemical Kinetics and Combustion, Novosibirsk, Russia, 1978. Led to eventual development of "Hydroscope" instrument over the next ten years.

First commercial instrument: IRIS Instruments in France imported Russian scientists and technology to develop NUMIS. Instrument uses coincident transmitter and receiver loops. Leased by Blackhawk for evaluation in Colorado and New Mexico.

Experimental Geometry

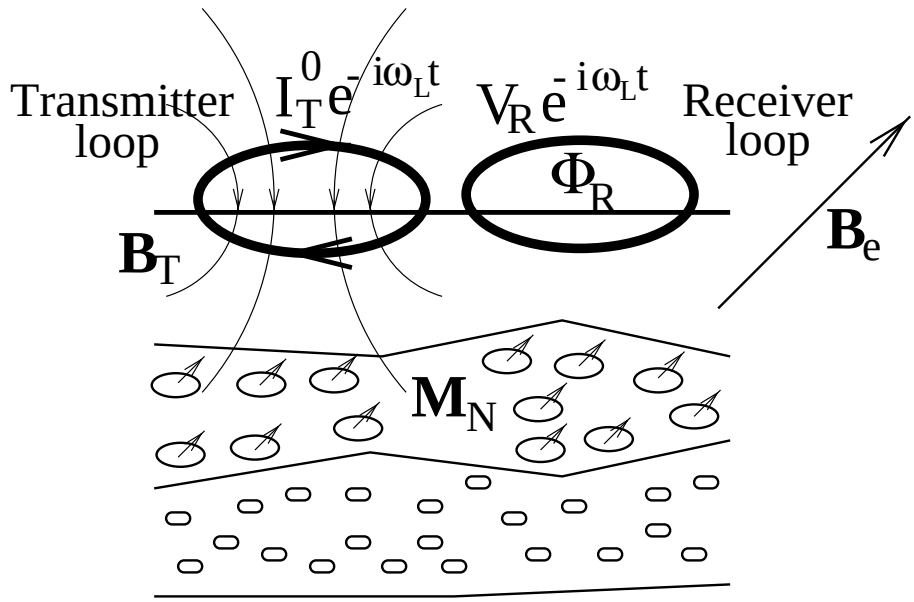

Basic Constraints

- Surface measurement $\Rightarrow$ Static field must be B_e
- Static field B_e $\Rightarrow$ Large sampling volume $\sim$ (100m)^3 required
- Receiver loop radius R_R $\Rightarrow$ Sampling volume $\propto R^3$, depth sensitivity $\propto R_R$
- Transmitter loop radius R_T $\Rightarrow$ $\mathbf{M}_N(\mathbf{r})$ is tipped significantly to depth $\propto R_T$
- Water sensitivity at $\sim$ 50m depth $\Rightarrow$ $R_R, R_T \sim$ 50m required as well!
- $0.01 \lesssim \omega_T/\omega_L \ll 1$ $\Rightarrow$ Transmitter loop current amplitude $I_T^0 \sim$ 300A

Happy window of intersection between technological requirements to obtain measurable signal and geophysical requirements for sensitivity to water at relevant depths

The Imaging Equation

Mathematical Ingredients:

I. Transmitter loop current $\mathrm{Re} I_T^0 e^{-i\omega_L t}$ $\Rightarrow$ Transmitted field in the conducting ground $\mathbf{B}_T(\mathbf{r}, t)$.

Standard approximation: Horizontally stratified Earth with piecewise constant conductivity, permeability.

Need to solve diffusion-dominated Maxwell Equations

$$\frac{1}{D}\partial_t \mathbf{A} \quad + \quad \nabla \times \left(\frac{1}{\mu}\nabla \times \mathbf{A}\right) = \frac{4\pi}{c}\mathbf{j}_T$$

$$\mathbf{B} \quad = \quad \nabla \times \mathbf{A}, \qquad D \equiv \frac{4\pi\sigma}{c^2}$$

Air

σ_1	μ_1
σ_2	μ_2
σ_3	μ_3
σ_4	μ_4

$\vdots$

Independent information on the Geoelectric section is not provided by the NMR signal, but must be provided by a complementary measurement (e.g., TDEM or FDEM sounding).

II. Co-rotating part $\mathbf{B}_T^+(\mathbf{r},t)$ of transmitter field $\Rightarrow$ Precessing in-plane magnetization $M_N^\perp(\mathbf{r},t) \propto \sin[\gamma|\mathbf{B}_T^+(\mathbf{r})|t]$

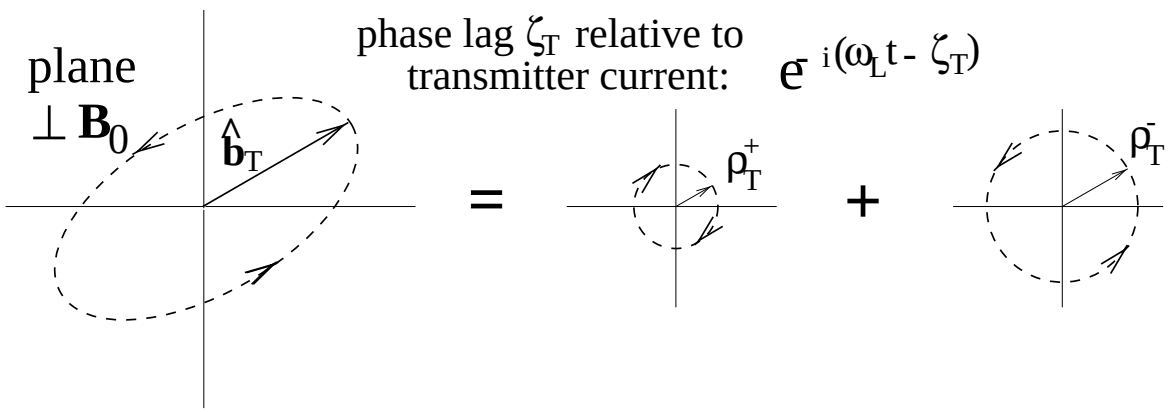

In general, projection of $\mathbf{B}_T^\perp$ of $\mathbf{B}_T$ into plane orthogonal to $\mathbf{B}_0$ is elliptically polarized, with semi-major axis $\hat{\mathbf{b}}_T$

$$\mathbf{B}_T^\perp(\mathbf{r},t) = \mathbf{B}_T^+(\mathbf{r},t) + \mathbf{B}_T^-(\mathbf{r},t)$$

$$\begin{cases} \mathbf{B}_T^+(\mathbf{r},t) & \text{rotates clockwise at } \omega_L \\ & |\mathbf{B}_T^+(\mathbf{r},t)| \equiv \rho_T^+ \\ \mathbf{B}_T^-(\mathbf{r},t) & \text{rotates counter clockwise at } \omega_L \\ & |\mathbf{B}_T^-(\mathbf{r},t)| \equiv \rho_T^- \end{cases}$$

Diffusive propagation $\Rightarrow$ time lag $\tau_{\text{diff}} \approx \frac{L^2}{D}$

$\Rightarrow$ Phase lag $\zeta_T(\mathbf{r})$ between transmitter current and co-rotating field:

$$I_T(t) = I_T^0 \cos(\omega_L t) \quad \Rightarrow \quad \mathbf{B}_T^+(\mathbf{r},t) \propto \cos[\omega_L t - \zeta_T(\mathbf{r})]$$

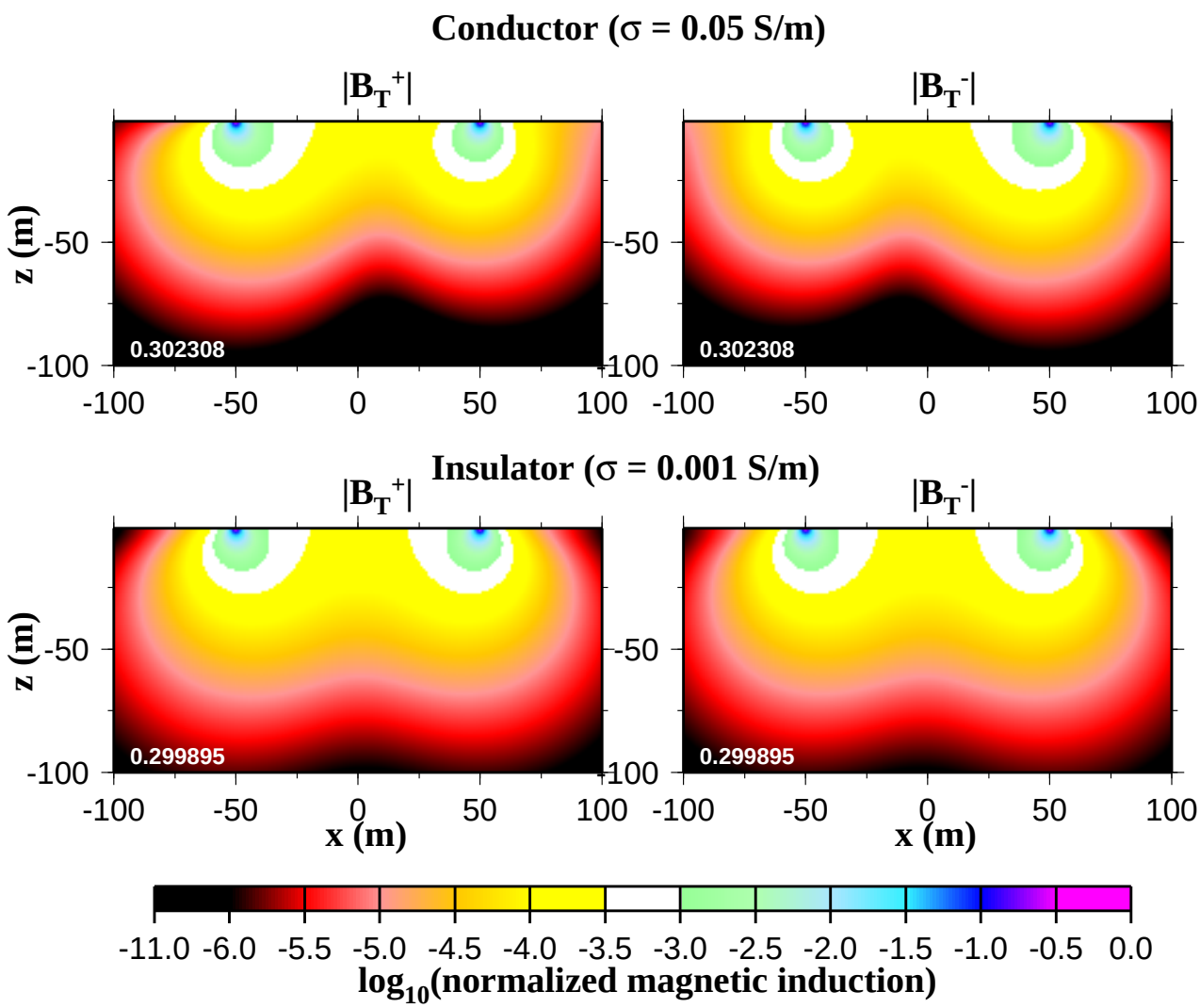

East-West oriented vertical slice of co-rotating and counter-rotating components of the field generated by a circular transmitter loop for insulating and conducting half-spaces. Asymmetry is due to the fact that $\mathbf{B}_e$ has been tilted 25° north from the vertical.

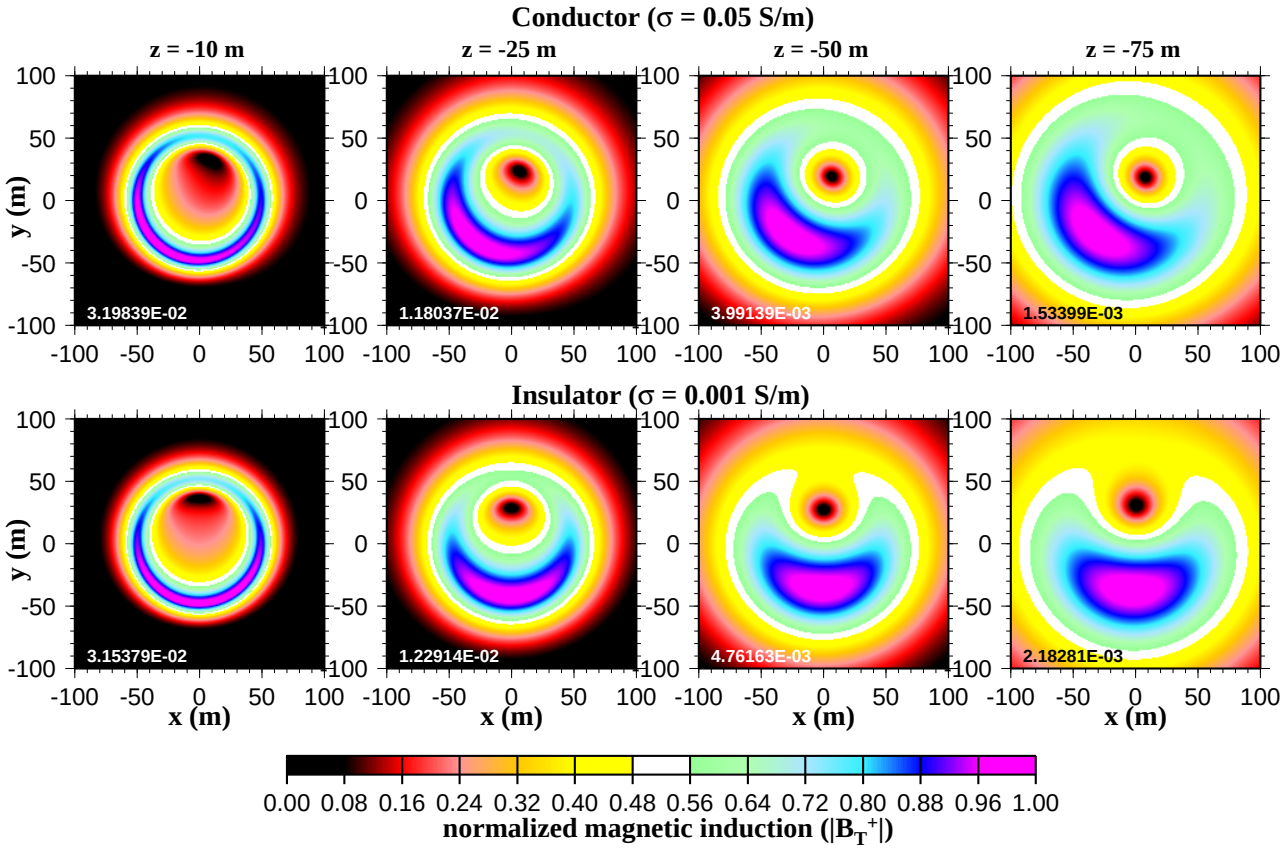

Same as previous slide, but now horizontal slices of the co-rotating and counter-rotating components of the transmitted field at various depths.

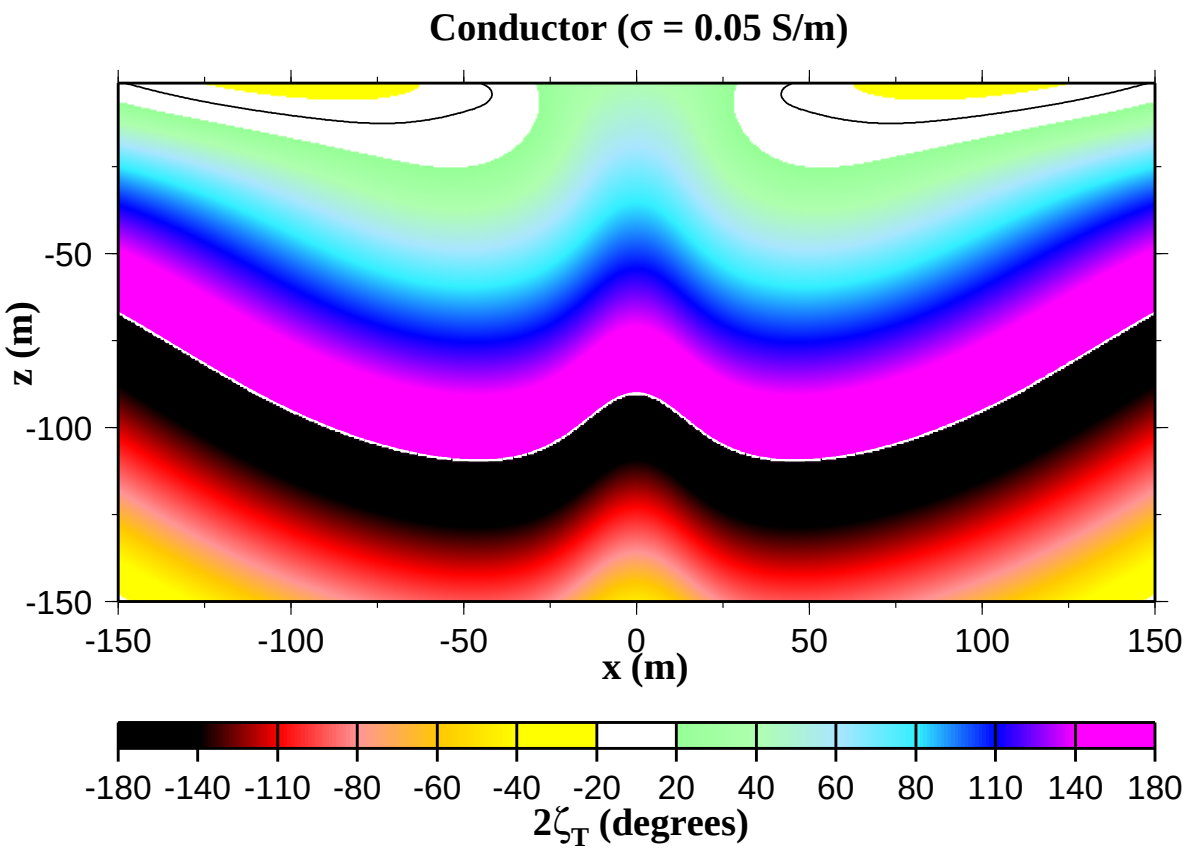

East-West oriented vertical slice showing the diffusive phase delay $\zeta_T(\mathbf{r})$ between the co-rotating field at depth in a conducting half-space, and the transmitter loop current at the surface. The central white line shows where the phase delay is 180°. The phase delay vanishes identically for an insulating half-space.

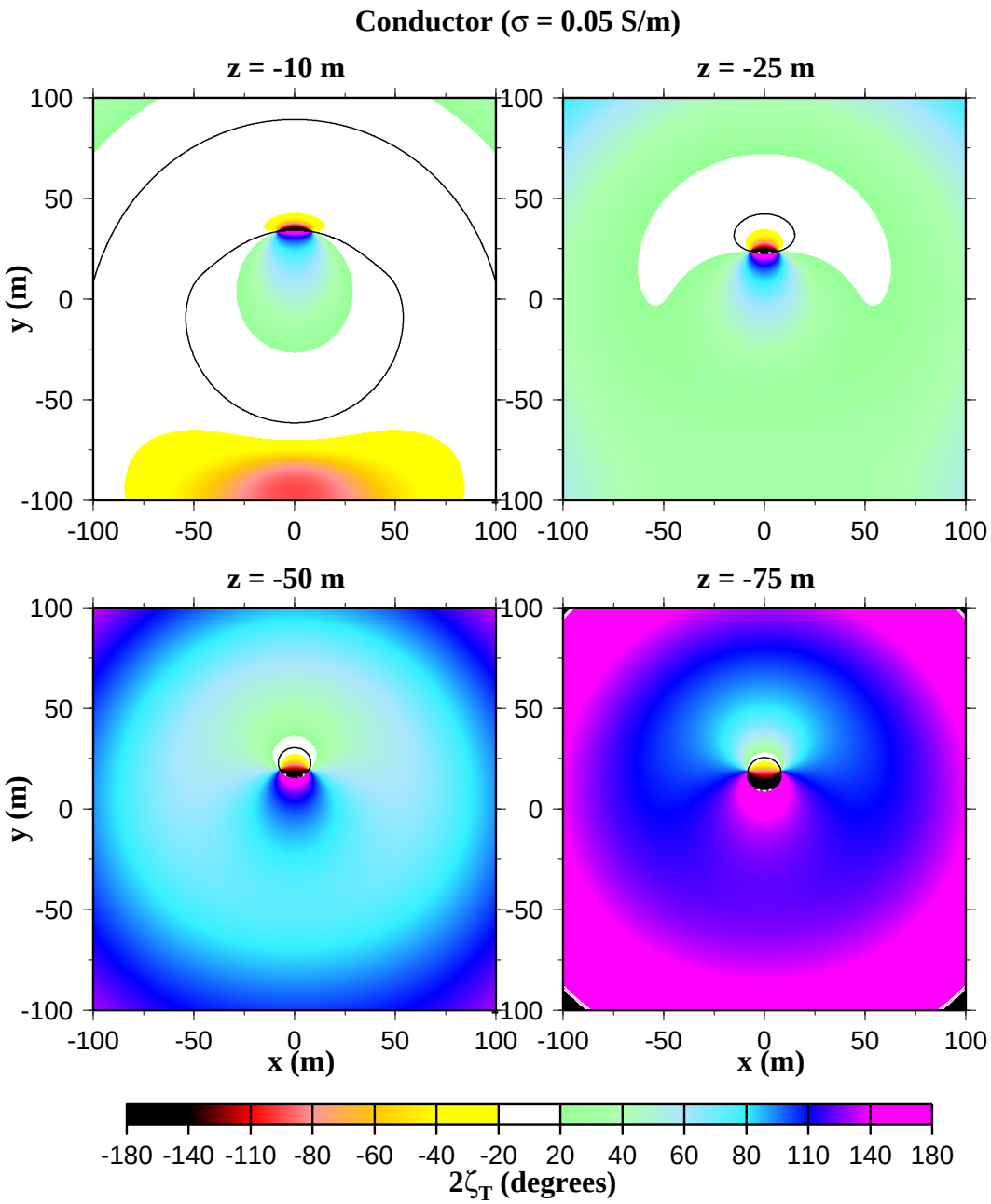

Same as previous slide, but now horizontal slices of the diffusive phase delay for various depths in a conducting half-space. The phase delay vanishes identically for an insulating half-space.

III. Precessing magnetization $\Rightarrow$ Nuclear magnetic field $\mathbf{B}_N(\mathbf{r},t)$.

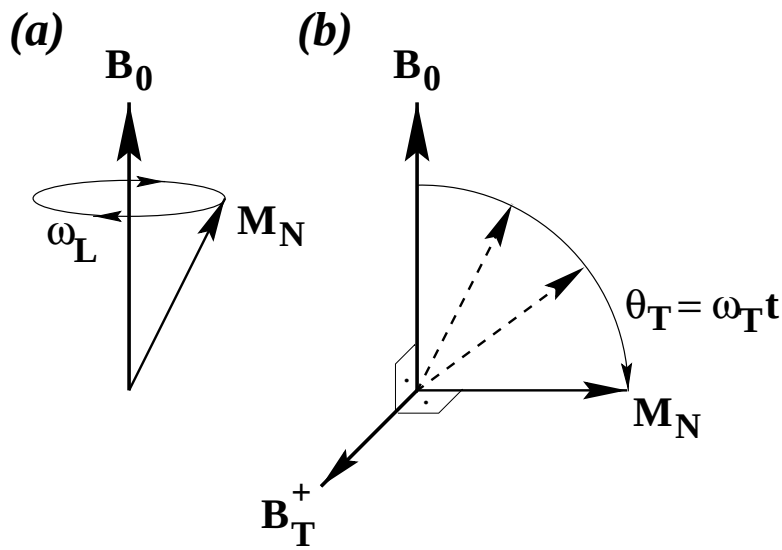

Maxwell Equations

$$
\begin{aligned}
\frac{1}{D}\partial_t \mathbf{A}_N \quad &+ \quad \nabla \times \left(\frac{1}{\mu}\nabla \times \mathbf{A}_N\right) = 4\pi \nabla \times \mathbf{M}_N \\
\mathbf{M}_N(\mathbf{r},t) \quad &= \quad \mathbf{M}_N^{(0)}(\mathbf{r}) \cos[\theta_T(\mathbf{r},t)] \\
&\quad + \; [\mathbf{M}_N^{(0)}(\mathbf{r}) \times \mathbf{B}_T^{+}(\mathbf{r},t)] \sin[\theta_T(\mathbf{r},t)] \\
\mathbf{B}_N \quad &= \quad \nabla \times \mathbf{A}_N, \qquad D \equiv \frac{4\pi\sigma}{c^2}
\end{aligned}
$$

Propagation of nuclear field back to receiver loop introduces a second phase lag.

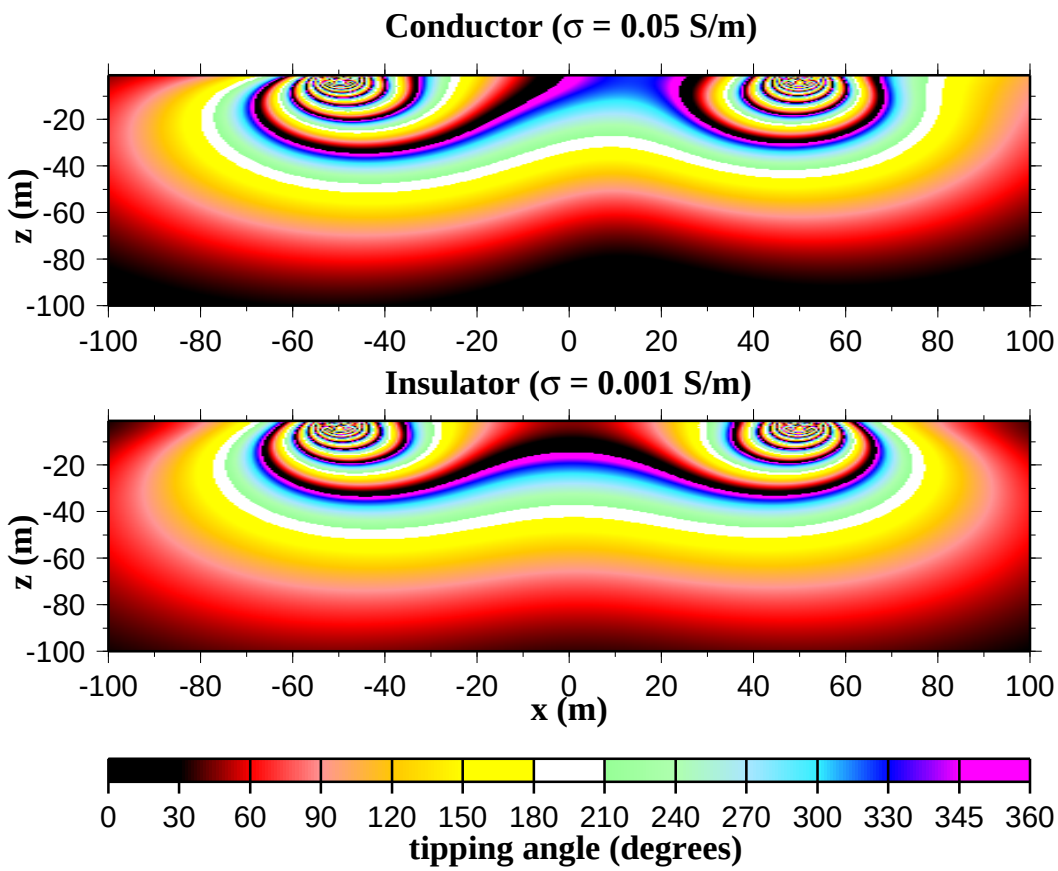

An East-West vertical slice of the tipping angle for an insulating and a conducting half-space for a relatively large pulse moment $q = 10^4$A-ms, which then places the lowest 90° tilt region about 70m below the surface.

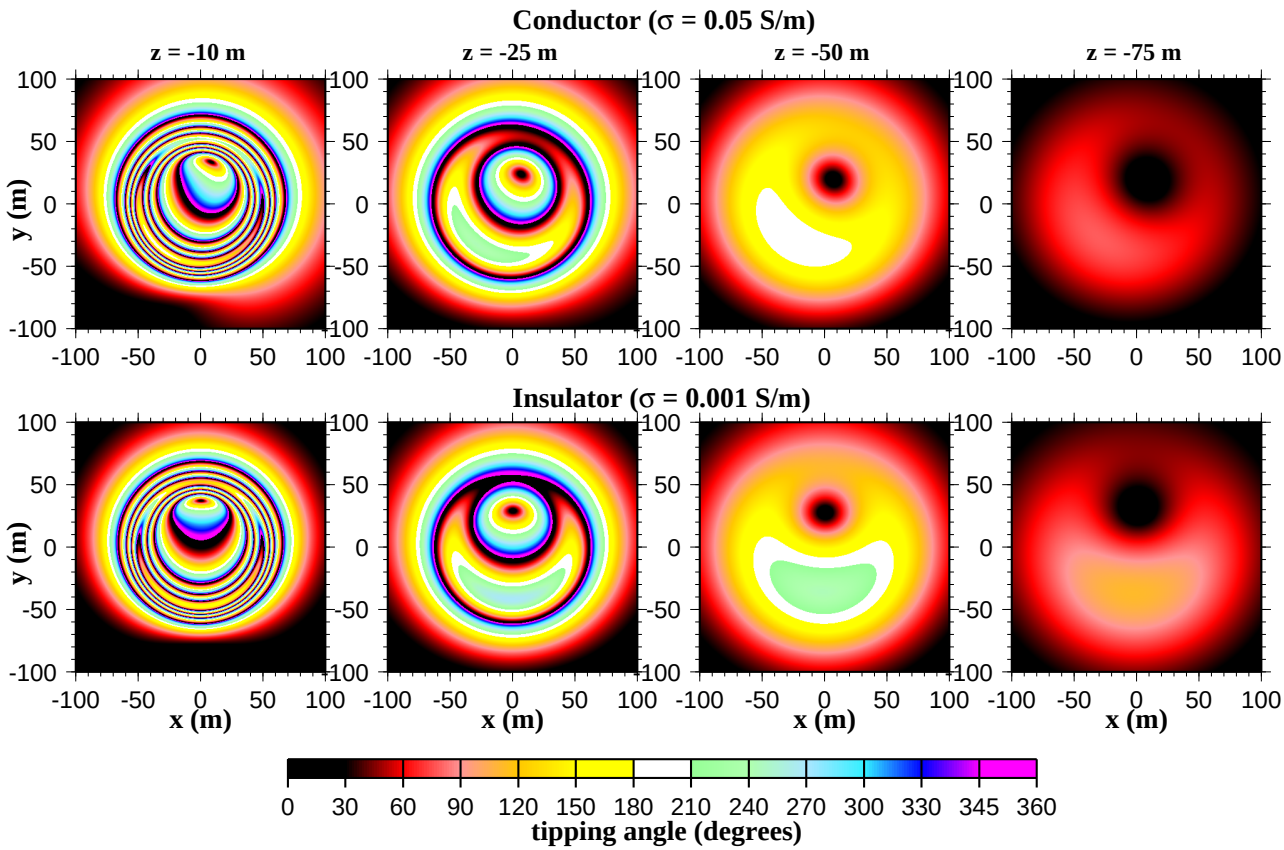

Same as previous slide, but now horizontal slices of the tipping angle at various depths.

IV. $V_R(t) = -\frac{1}{c}\frac{d\Phi_R}{dt}$ Faraday Law of Induction: Time varying flux through receiver loop $\Rightarrow$ Receiver loop voltage with nuclear contribution

$$\Phi_R^N(t) = \int_{\Sigma_R} \mathbf{B}_N(\mathbf{r},t)\cdot\hat{\mathbf{n}}d\Sigma$$

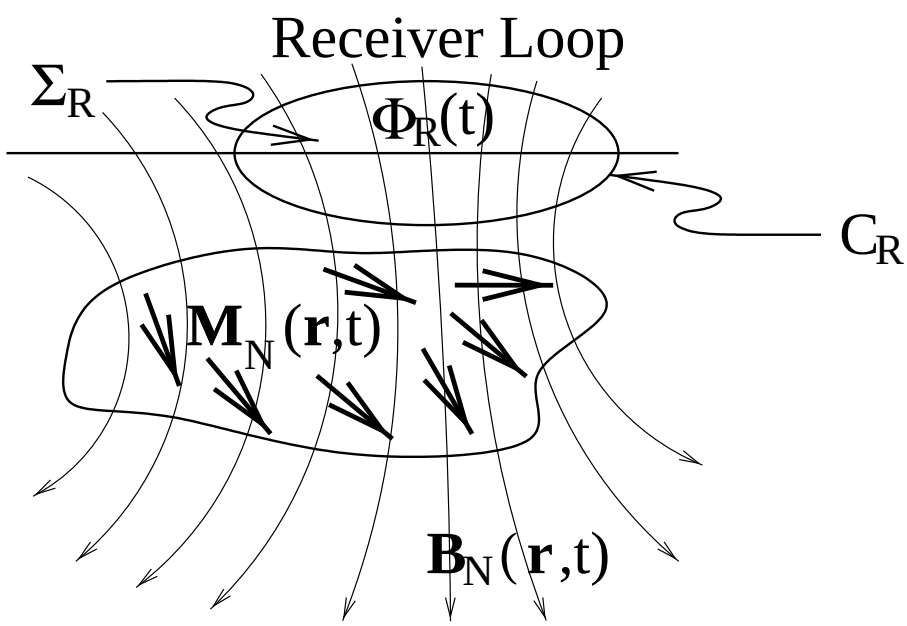

Final Imaging Equation

Incorporating ingredients I, II, III, IV and blending well, one obtains for the amplitude and phase of the NMR receiver voltage

$$V(q, \mathbf{x}_0) = \int d^3r K(q, \mathbf{x}_0; \mathbf{r}) n_N(\mathbf{r})$$

$$K(q, \mathbf{x}_0; \mathbf{r}) = -\frac{2\gamma^2 \omega_L S(S+1) B_0}{3k_B T} \sin\left[\gamma q \rho_T^+(\mathbf{r})\right] \rho_R^-(\mathbf{r})$$

$$\times \; e^{i[\zeta_T(\mathbf{r}) + \zeta_R(\mathbf{r})]} \left[\hat{\mathbf{b}}_R(\mathbf{r}) \cdot \hat{\mathbf{b}}_T(\mathbf{r}) + i\hat{\mathbf{B}}_0 \cdot \hat{\mathbf{b}}_R(\mathbf{r}) \times \mathbf{b}_T(\mathbf{r})\right]$$

$q = I_T^0 \tau_p$ "pulse moment"

$\mathbf{x}_0 =$ apparatus horizontal position

$\rho_R^{\pm}(\mathbf{r}), \hat{\mathbf{b}}_R(\mathbf{r}), \zeta_R(\mathbf{r}) =$ elliptical decomposition of $\mathcal{B}_R$

For coincident transmitter and receiver loops:

$$K(q, \mathbf{x}_0; \mathbf{r}) = -\frac{2\gamma^2 \omega_L S(S+1) B_0}{3k_B T} e^{2i\zeta_T(\mathbf{r})} \rho_T^-(\mathbf{r}) \sin\left[\gamma q \rho_T^+(\mathbf{r})\right]$$

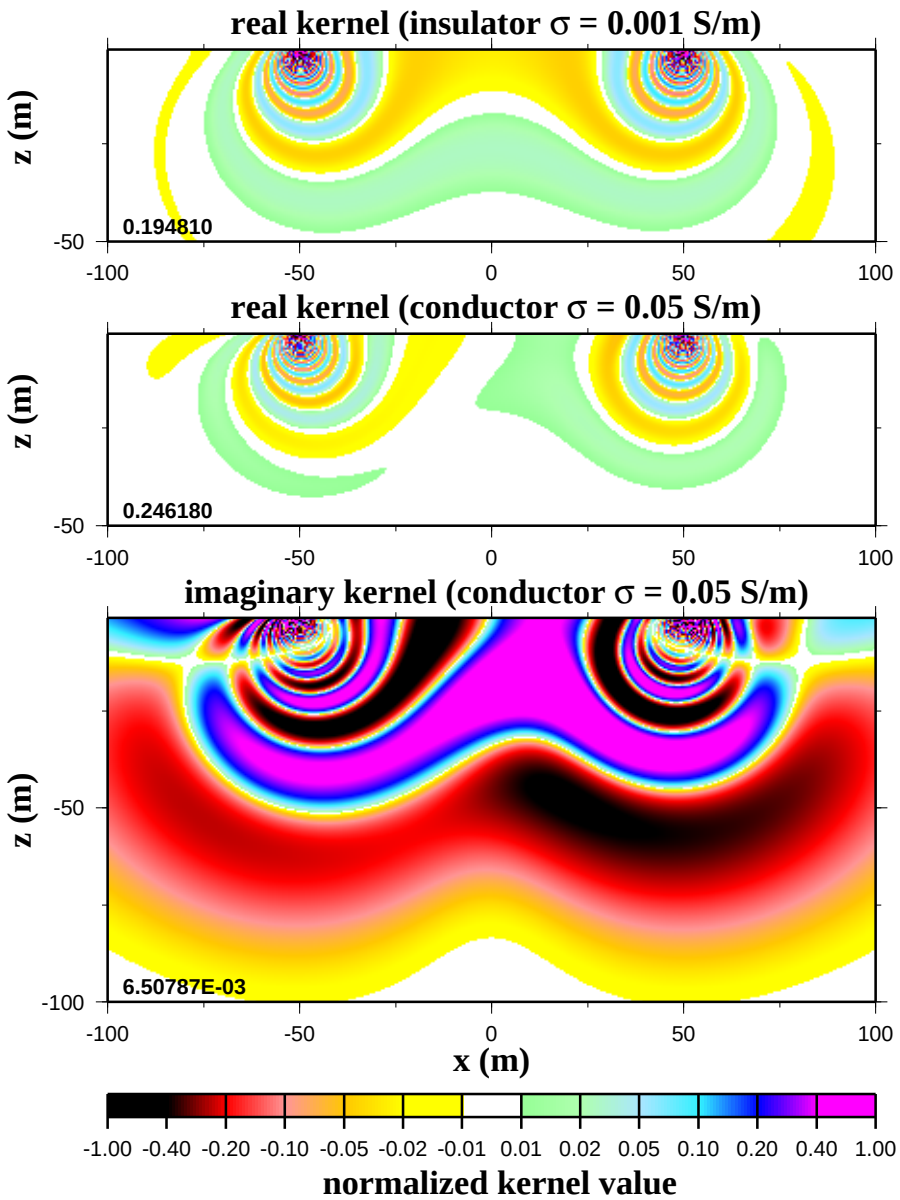

An East-West vertical slice of the three-dimensional imaging kernel for conducting and nonconducting half-spaces. The imaginary part vanishes identically for the insulating case. The pulse moment has been chosen to be $q = 10^4$A-ms.

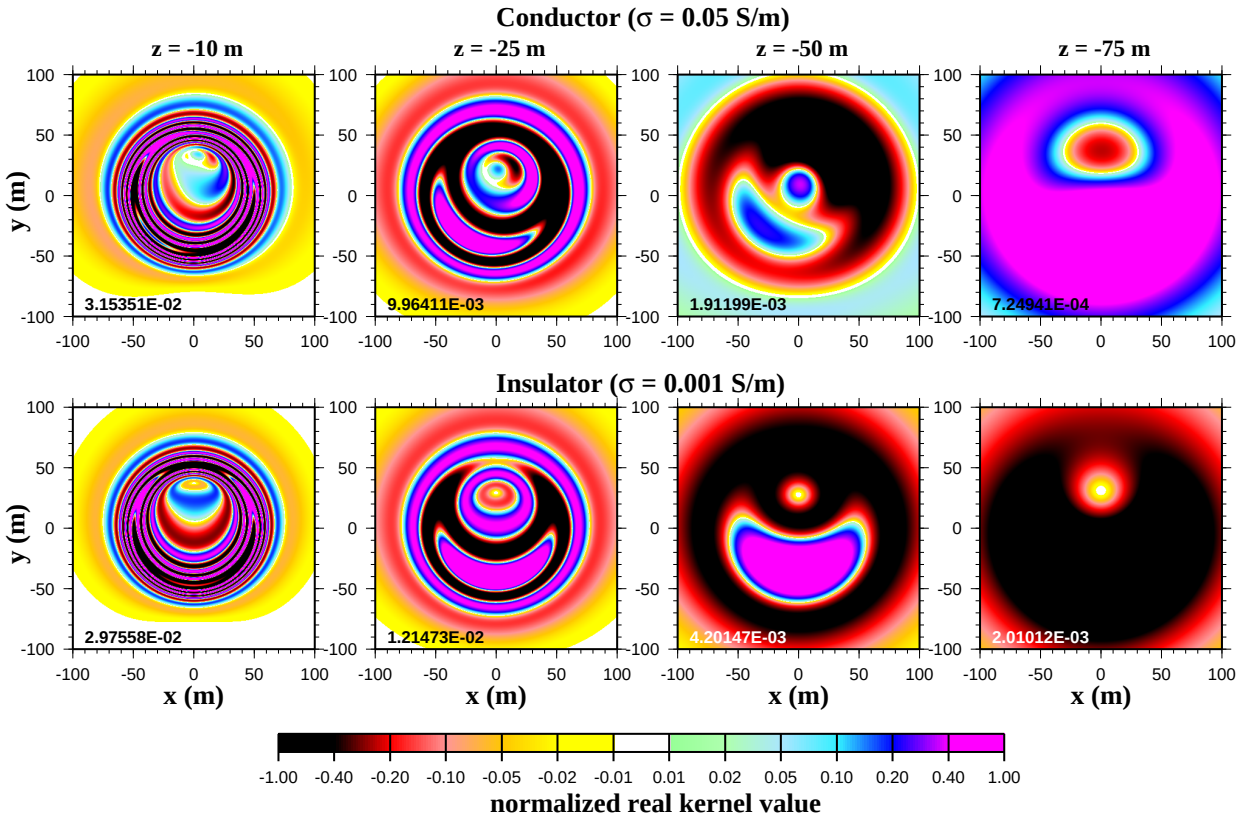

Same as previous slide, but now horizontal slices of the real part of the imaging kernel at various depths for conducting and insulating half-spaces.

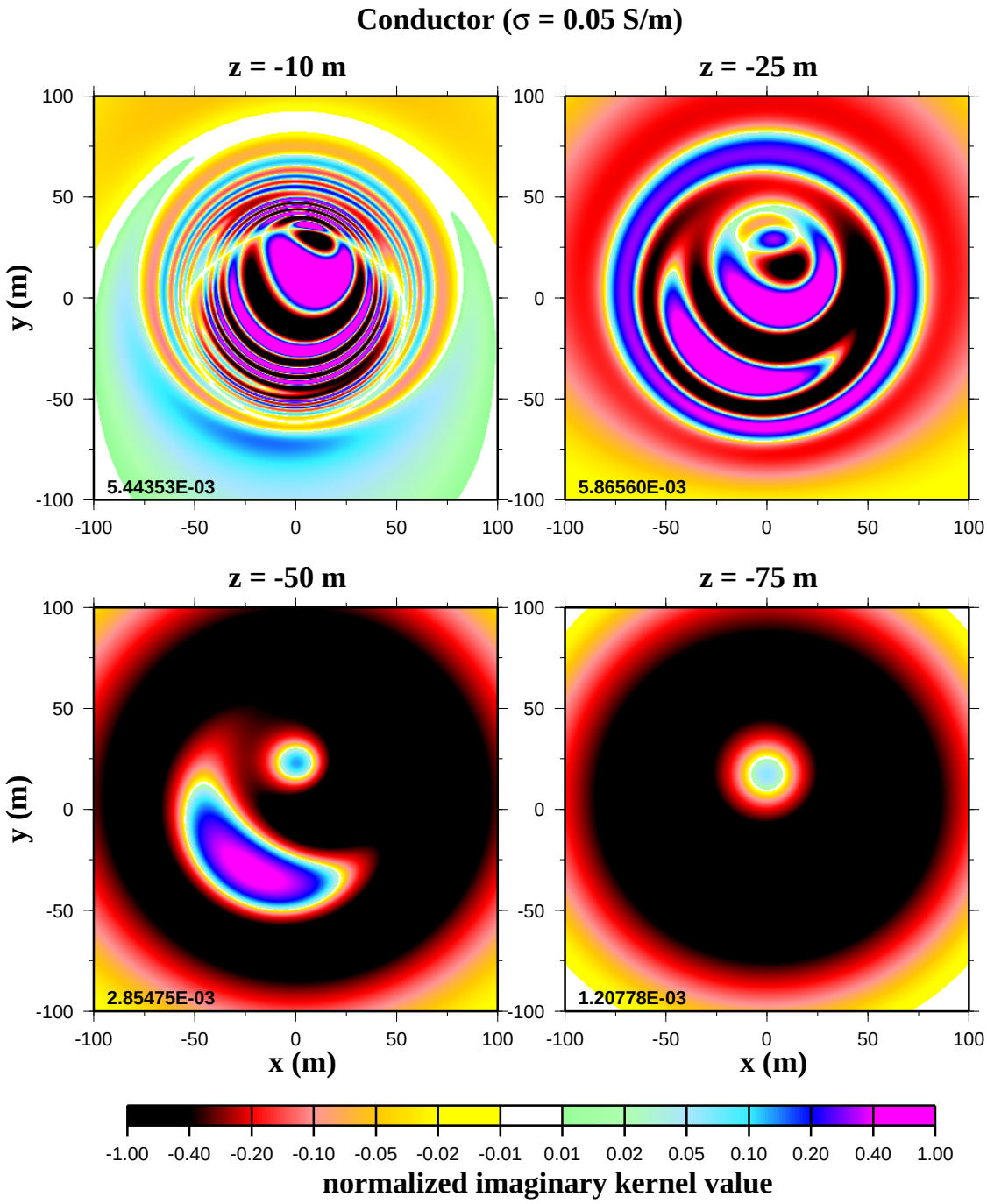

Same as previous slide, but now horizontal slices of the imaginary part of the imaging kernel at various depths for conducting half-space. The imaginary part vanishes identically for an insulating half-space.

Relaxation and Porosity

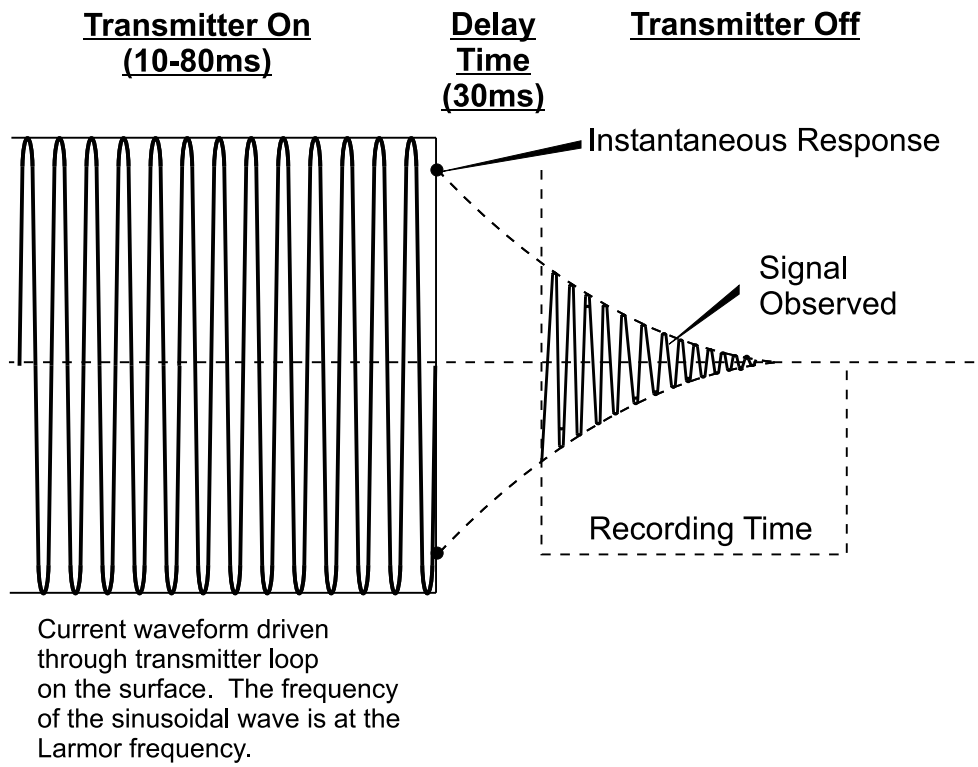

In fact, the NMR signal contains more than just information about the water distribution.

NMR signal relaxation time T_2 contains information about the subsurface physical and chemical environment.

$$V(q, \mathbf{x}_0; t) = \int d^3r K(q, \mathbf{x}_0; \mathbf{r}) n_N(\mathbf{r}) e^{-t/T_2(\mathbf{r})}$$

$$\partial_t V(q, \mathbf{x}_0; t = 0) = -\int d^3r K(q, \mathbf{x}_0; \mathbf{r}) \frac{n_N(\mathbf{r})}{T_2(\mathbf{r})}$$

Magnetic impurities in the porous rock dominate relaxation, leading to dephasing and spin flips.

$$\frac{1}{T_2} = \rho_2 \frac{S}{V}$$

- "Surface relaxivity" $\rho_2 \propto$ impurity concentration and magnetic reactivity
- S/V surface-to-volume ratio of pores (larger for small pores)
- Kozeny equation for "Hydraulic permeability":

  $$k \propto \phi^3 (S/V)^{-2}, \quad \phi = \text{porosity}.$$

  Of fundamental interest for oil extraction and toxic spill remediation

Practically, due to 30ms instrumental delay time, water in very fine pores, or in highly magnetic soils, is simply invisible. This, together with cultural noise, is the strongest limitation on use of the present instrument.

The Inverse Problem

Inferring water distribution from NMR signal

Recall

$$V(q, \mathbf{x}_0) = \int d^3r K(q, \mathbf{x}_0; \mathbf{r}) n_N(\mathbf{r}).$$

To obtain full three-D $n_N(\mathbf{r})$, need three experimental degrees of freedom.

Presently, apparatus is too bulky for convenient variation of horizontal position $\mathbf{x}_0$. Instead, approximate water distribution as horizontally stratified, and vary pulse moment $q = I_T^0 \tau_p$ only

$$\begin{aligned} V(q) &= \int dz \bar{K}(q; z) n_N(z) \\ \bar{K}(q; z) &\equiv \int dx dy K(q, \mathbf{x}_0; x, y, z). \end{aligned}$$

This is "simple" one-dimensional, linear, matrix inverse problem.

Unfortunately, due to rapid decay of the sensitivity with depth, the problem is very poorly conditioned, and various regularization techniques, based on physically motivated prior constraints, must be employed.

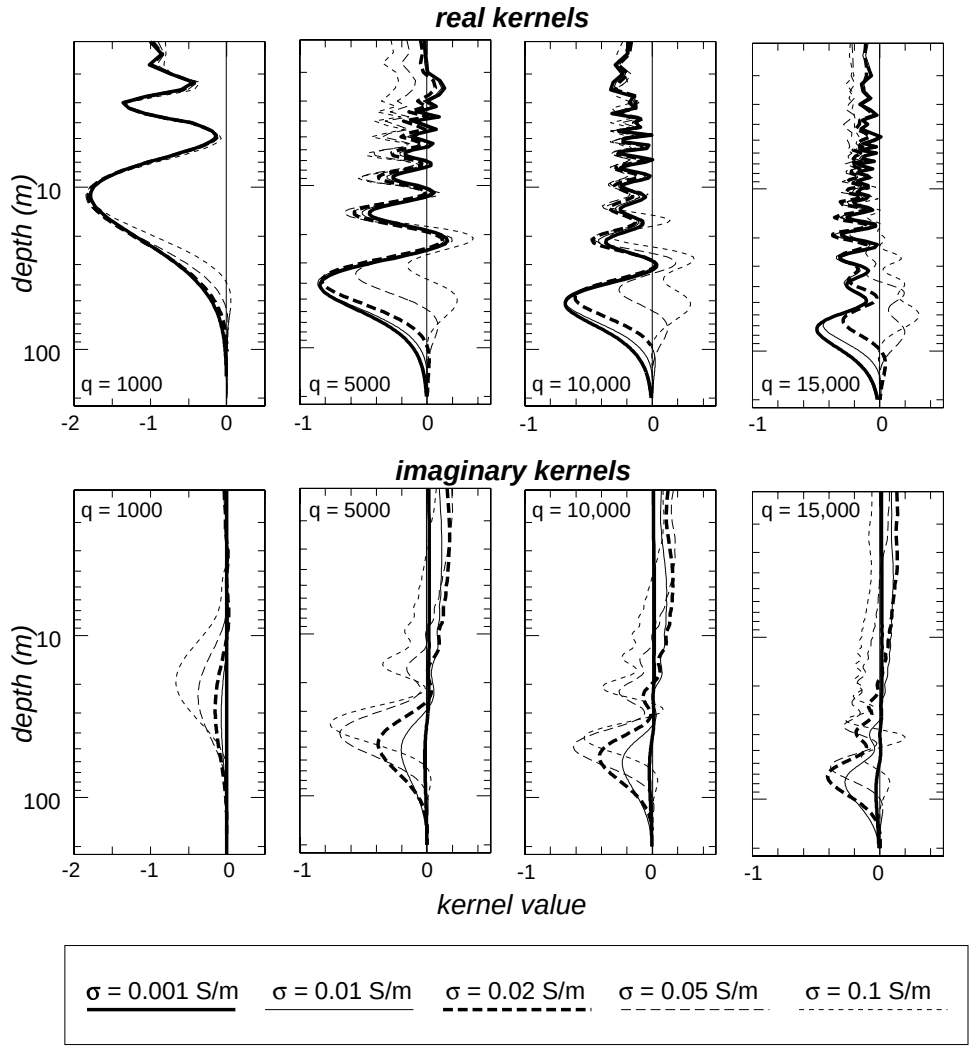

Real and imaginary parts of the horizontally integrated, effectively one-dimensional kernels for various pulse moments and various half-space resistivities in the range $10\Omega\text{m} \leq \rho_{\text{dc}} \leq 1000\Omega\text{m}$. Notice that the imaginary part appears to focus on a well defined depth range that increases with increasing q, whereas the real part has a more oscillatory structure. At depth, insulating and conducting real kernels are *opposite in sign* due to the phase delay effect.

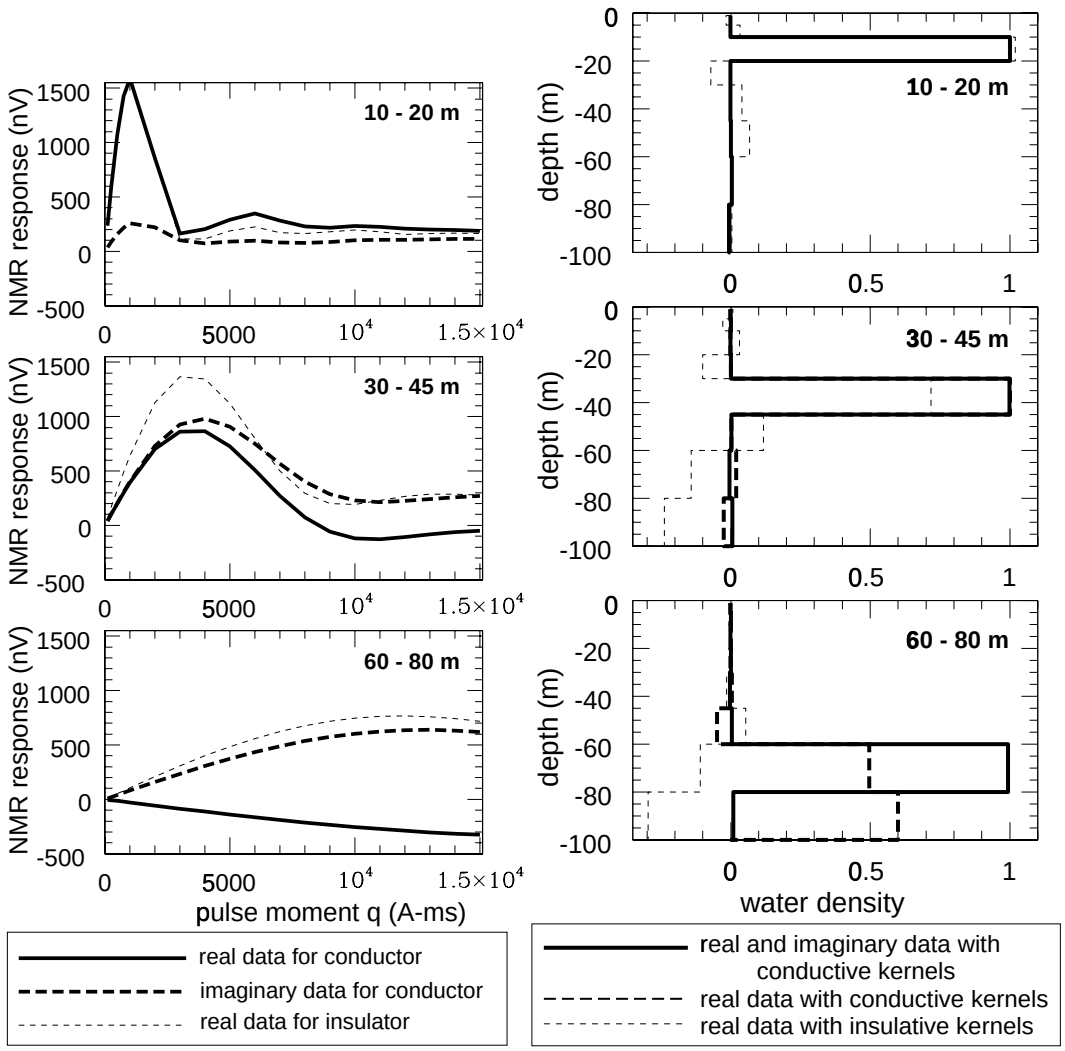

Left: synthetic forward data, $V(q)$ for conducting, $\rho_{\text{dc}} = 20\Omega\text{m}$, and insulating half spaces, in which a single layer of bulk water is present at varying depths.

Right: inversions of synthetic forward data for the conducting half-space using (a) both real and imaginary parts of the data, (b) only the real part of the data, and (c) the real part of the data using the incorrect insulating kernel. The latter yields ever more spurious results as the depth increases.

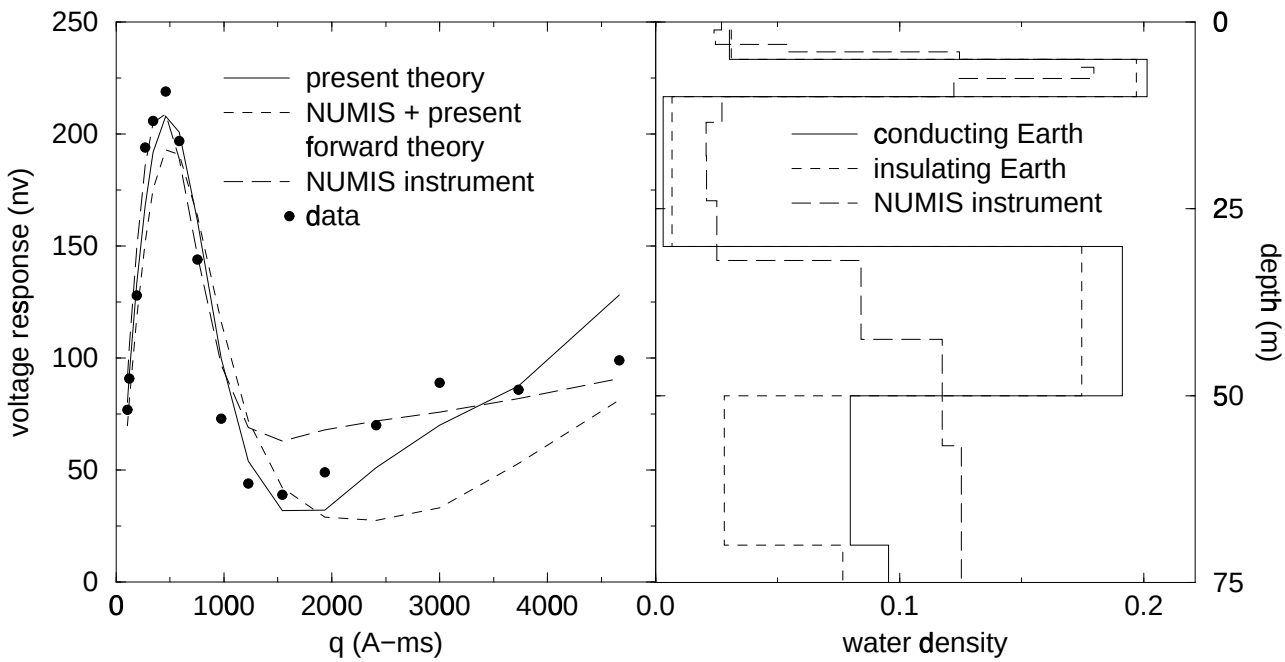

Measured NMR signal (left) and derived water content distribution (right) at Cherry Creek site in the Denver area. Black squares on the left are experimental data. Long-dashed line on the right is the inversion obtained by NUMIS using the Earth model $\rho = 15\Omega$m, 25Ωm, and 10Ωm in layers 0-10m, 10-20m, and below 20m, respectively. Solid and short-dashed lines are our inversions based on this same Earth-model, and on an insulating Earth, respectively. Solid line on the left is the predicted voltage from our inversion; long-dashed line is the NUMIS result; short-dashed line is our prediction from the NUMIS inversion.

Conclusions
Pros and Cons

- Unlike purely EM methods NMR signal represents an essentially *unique* of the presence of water protons.

- The theoretical underpinnings of the NMR technique now rest on solid ground.

- Unlike borehole methods, surface NMR method is non-invasive, and hence avoids contact with contaminated soil.

- NMR method works poorly under less than ideal conditions where many important applications lie. Presently limited to unpopulated regions with magnetically clean soils.

- Measurement protocol is time consuming (e.g., locating ω_L to within $\sim 1\%$ takes several hours) due to limitations of power source (car batteries).

Future Improvements

- Shorten dead time from transmit to receive status from 30ms to a few ms
- Improved noise reduction: Better Frequency filtering? Better loop geometries?
- Replace battery power source by a (quiet!) higher voltage source (would allow lighter cables, and would speed up measurement protocol)

The next generation of instrument may emerge from a Blackhawk-NASA/JPL collaboration that is proposing a robotic surface NMR instrument to search for water on Mars. Other funding will be required, however, to transfer the new technology to an Earth based system.

NMR dowsing holds great potential promise, but is a technology still in its infancy

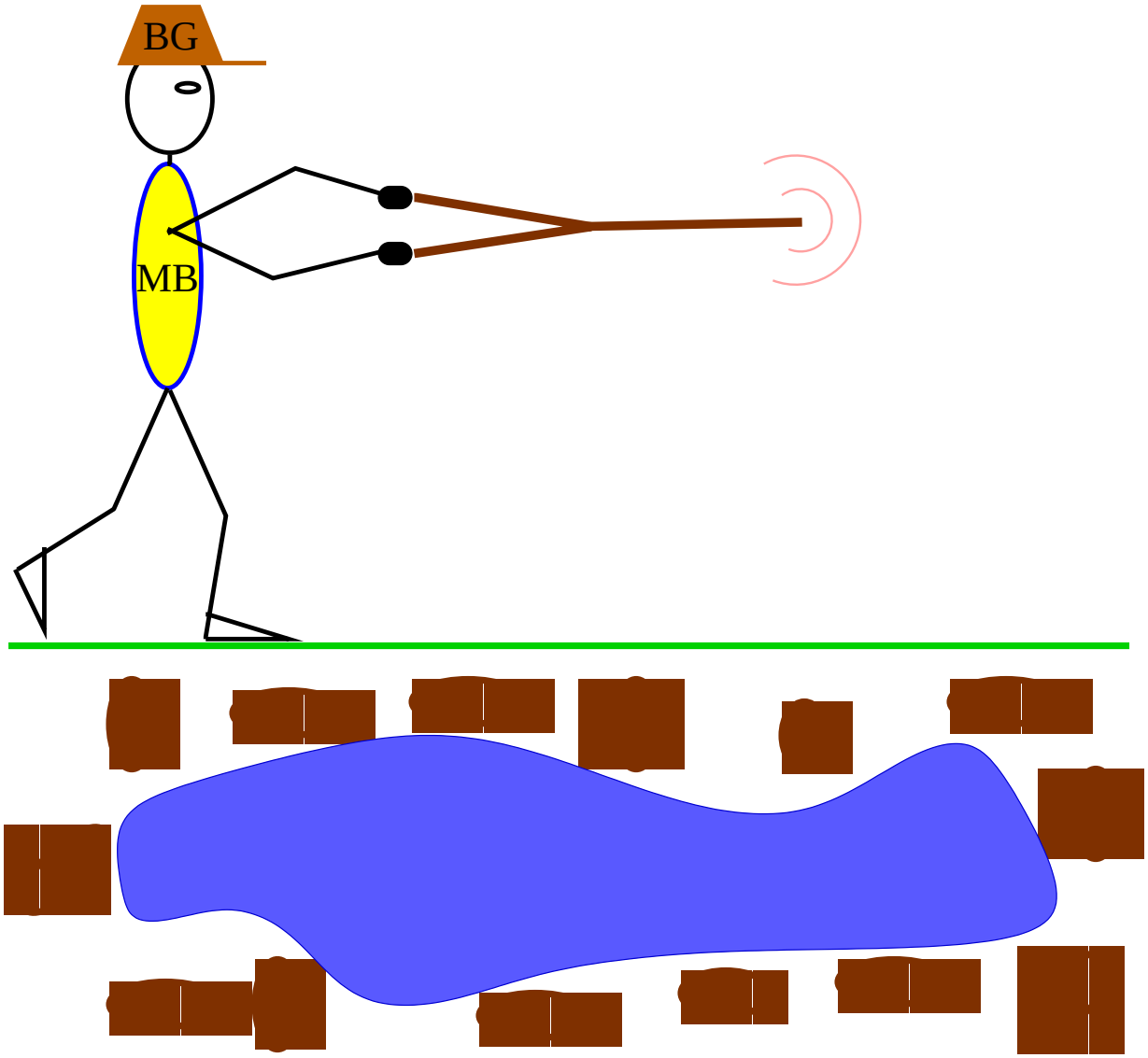

It nevertheless represents an improvement over certain other non-invasive techniques